Modeling excitable media by a one variable cellular automaton: Application to the cardiac case

A. Giaquinta, S. Boccaletti,[a] L. Tellini,[b] and F. T. Arecchi[a]
Istituto Nazionale di Ottica, Largo E. Fermi, 6, I50125 Florence, Italy

(Received 20 April 1994; accepted for publication 12 July 1994)

The dynamics of an assembly of cardiac cells is modeled by a simple cellular automaton that reduces to a single variable the two variable competition of the standard models of excitable media. Furthermore, a short superexcitability period is introduced, as suggested by the dynamics of the single cardiac miocyte. The model reproduces several pathological cardiac behaviors as, e.g., the fast transition from normal behavior to fibrillation, showing how this latter one can either occur over the whole spatial domain or can be confined within a limited region.

In the last decade analysis and simulation of excitable media (EM) has been developed in order to describe a variety of different physical situations like chemical reactions (e.g. Belouzov–Zhabotinsky reaction,[1,2] cardiac behavior,[3–5] competition and dynamics of biological species (biochemical activity of *Dictyostelium discoideum*) and propagation of infection in biological populations.[6]

EM dynamics is ruled by two coupled nonlinear reaction diffusion equations, which predict a large number of spatiotemporal phenomena for different selections of control parameters. A complete classification of the different behaviors emerging from them is given by Kerner and Osipov (KO).[7] In particular, temporal and spatial scales play a fundamental role in producing stationary spatial or Turing instabilities (K-systems), uniform temporal or Hopf instabilities (Ω-systems) and spatiotemporal or Turing–Hopf instabilities ($K\Omega$-systems). Calling u and v the concentrations of the two reacting species, τ_u and τ_v the corresponding damping times and l_u, l_v their diffusion lengths, the KO classification permits us to discriminate situations in which either the reaction times (Ω-systems) or the diffusion lengths (K-systems) or both ($K\Omega$-systems) are very different from one another.

In many physical, biological and chemical situations, reaction diffusion kinetics has been treated by cellular automata (CA),[2,8] coupled map lattices,[9] or by direct numerical simulations of the partial differential equations (PDE).[10]

In this paper we deal with the particular situation in which the reaction-diffusion system has the two time scales very different so that $\varepsilon \equiv \tau_u/\tau_v$ is close to zero.[6,11] In such a case we can describe the evolution of the two reacting species by a single global variable which accounts for all the relevant dynamical properties of the system. To simulate the spatiotemporal evolution of this single variable we build a new CA model whose rules can be easily inferred as the $\varepsilon \to 0$ limit of a two variable model.

In order to apply our results to the dynamics of a cardiac tissue we will refer to the FitzHugh–Nagumo (FHN) model[3] enriched by the further introduction of a short superexcitability time interval, the experimental evidence of which has been recognized in several circumstances.[12] As we will see, this extra period is crucial in order to simulate a fast transition from plane waves to spatially and temporally decorrelated patterns. This situation corresponds to the induction of the fibrillation via a single extra stimulus.[13]

Let us consider a reaction diffusion system described by

$$\tau_u \frac{\partial u}{\partial t} = l_u^2 \nabla^2 u + f(u,v),$$

$$\tau_v \frac{\partial v}{\partial t} = l_v^2 \nabla^2 v + g(u,v), \tag{1}$$

where u and v are the concentrations of two competing species, τ_u and τ_v are the corresponding reaction times, l_u and l_v the diffusion lengths and $f(u,v)$, $g(u,v)$ two nonlinear functions. Calling $\varepsilon = \tau_u/\tau_v$, we rescale space and time as follows:

$$t \to t/\tau_v,$$

$$(x,y) \to \left(\frac{\varepsilon x}{l_u}, \frac{\varepsilon y}{l_u}\right), \tag{2}$$

and assume to have a nondiffusive v variable ($l_v = 0$). The above system can be rewritten as

$$\varepsilon \partial_t u = \varepsilon^2 \nabla^2 u + f(u,v),$$

$$\partial_t v = g(u,v). \tag{3}$$

We specify the analytical form of the two coupling functions by a modified FHN model[4,9] with piecewise linear functions of the form

$$f(u,v) = u(u-1)\left(q + \frac{1-q}{M} v - u\right),$$

$$g(u,v) = G((M+1)u - v). \tag{4}$$

The nullclines $f(u,v)=0$ and $g(u,v)=0$ are shown in Fig. 1. The curve $f(u,v)=0$ consists of an upper (f_+) and a lower (f_-) branch connected by the unstable ($\tilde{f}$) branch, and $g(u,v)=0$ is a single straight line. The constant q represents the excitation threshold of the rest state ($u=0, v=0$), M is the v value at which intersection between the branches f_+ and $\tilde{f}$ occurs; $G \in (0,1)$ is a suitable constant to be specified later.

Looking at Eqs. (3) as well as at Fig. 1, the limit $\varepsilon \to 0$ reduces the first equation to $f(u,v)=0$ and the instability of

[a]Also at Department of Physics, University of Florence, Florence, Italy.
[b]Also at Department of Cardiology, S. Donato Hospital, Arezzo, Italy.

 1054-1500/94/4(3)/557/5/$6.00

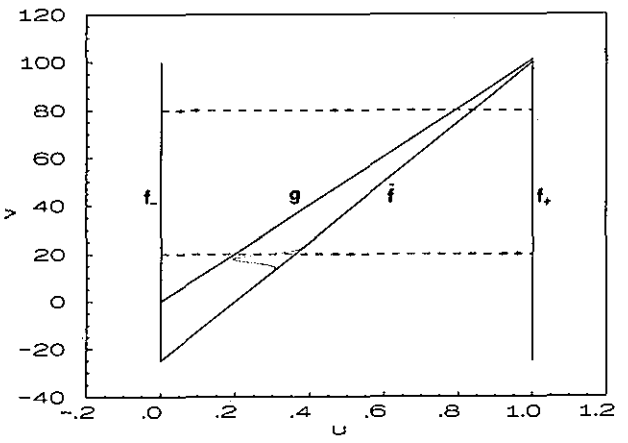

FIG. 1. Nullclines from Eq.(4) in the phase plane (u,v) for the reaction diffusion system (1) with $M=100$, $q=0.2$. $f_{\pm}$ are the stable branches, $\tilde{f}$ is the unstable one. The oriented dashed lines represent the minimal excitation cycle for transition levels $\sigma_e=20$ (upward) and $\sigma_d=80$ (downward), where σ is a local coordinate along the $f_{\pm}$ branches, defined by Eq. (5). The thin line is a qualitative scheme of the superexcitability modification introduced in Eq. (12) ($C_1=0.15, C_2=5$).

the $\tilde{f}$ branch strictly slaves the u variable to assume only the two integer values 0 (unexcited state) and 1 (excited state). As for the v variable, it ranges from 0 to its maximum value M. Furthermore, the $\varepsilon \to 0$ limit implies that the u variable has a characteristic time scale much faster than that of the v variable. In such a case we can study the evolution of the system making reference to the time scale of the slow variable. This means that, referring to a discrete time model with a temporal updating step $\Delta t > \tau_u$, we must assume that the system instantaneously jumps from the excited to the unexcited branch of $f(u,v)=0$ and vice versa without changes in the v variable. In other words, on a single temporal step u passes from 0 to 1 or from 1 to 0 with the same associated v. Therefore the dynamics develops only inside the two stable branches of the nullcline $f(u,v)=0$.

Such a circumstance permits us to define the new global variable

$$\sigma = |2Mu - v|, \tag{5}$$

which univocally determines the dynamical state of the system. Calling respectively $\sigma_{\pm}$ the analytical expressions of the new variable inside the branches $f_{\pm}$, we have

$$\sigma_+ = 2M - v, \quad \sigma_- = v, \tag{6}$$

and correspondingly

$$\frac{d}{dt}\sigma_{\pm} = \pm G_{\pm}(v - (M+1)u), \tag{7}$$

where $G_{\pm}$ are two different constants associated with the branches $f_{\pm}$. We choose $G_+ > G_-$ to account for a shorter permanence in f_+ with respect to that in f_-. Specifying Eq.(7) on the two branches we have

$$\frac{d}{dt}\sigma_+ = G_+(M-1-\sigma_+),$$

$$\frac{d}{dt}\sigma_- = -G_-\sigma_-. \tag{8}$$

With this in mind, we construct a CA model assigning to σ an integer value ranging from 0 to $2M$ with the following stipulations: for $\sigma < \sigma_e$ the system is in an excitable state (low state, transition allowed); for $\sigma_e \leqslant \sigma < M$ the system is in an absolute refractory state (low state, transition forbidden); for $M < \sigma \leqslant 2M - \sigma_d$ the system is in a "de-excitable" state (upper state, transition allowed) and finally for $2M - \sigma_d < \sigma \leqslant 2M$ the system is in a stable excited state (downward transition forbidden). Here we have introduced two levels (σ_d and σ_e) to discriminate the situation in which transitions between the two stable branches can occur. In cardiologist jargon the time interval spent in the low branch f_- below (respectively above) σ_e is called "relative (respectively absolute) refractory period." To avoid confusion with the period of a wave (ratio between its wavelength and its velocity), in this paper we will name these "periods" as intervals.

The σ variable is defined on a grid of $N \times N$ squares, each square housing a point cell at a random position within it.[2] The cell position is determined once forever with the further assumption that two cells must be separated by more than a minimal distance $r_{\min}$.[14] In such a way a satisfactory homogeneity among all the spatial directions is obtained (for the simulations we have chosen $r_{\min}=0.6$). We have set no flux boundary conditions. The diffusion acting on the u variable is taken into account (as in all previous CA models) by defining a neighborhood $\mathscr{S}$ of the single cell over which the Laplacian is effective. We choose as neighborhood of a cell the set of those cells separated by less than a fixed interaction radius R and assume that diffusion provides equal contributions δ from each excited cell falling within $\mathscr{S}$. In fact, a better approximation of the effect of the Laplacian term in Eq. (3) is provided by a finite difference equation.[9] This improvement will be extensively treated in a forthcoming paper. In our model we assume δ equal to the reciprocal of the averaged total number of cells ($\langle N_{\text{tot}} \rangle$) falling inside $\mathscr{S}$. On the other hand, this last quantity is equal to $a-1$ (a being the area of the neighborhood).

Calling respectively N_e (N_d) the total number of excited (unexcited) cells falling inside $\mathscr{S}$ ($N_e + N_d = N_{\text{tot}}$), the total contribution due to the diffusive interaction is $N_e/(a-1)$ for an unexcited cell and $-N_d/(a-1)$ for an excited one.

With this in mind, for each i, j, the evolution rules for the σ variable read as

$$\sigma_{i,j}(t+1) = 2M - \sigma_{i,j}(t) \tag{9}$$

if $\sigma_{i,j}(t) < \sigma_e$ and $N_e > p + (a-1-p)[\sigma_{i,j}(t)/M]$, or if $M < \sigma_{i,j}(t) \leqslant 2M - \sigma_d$ and $N_d > (a-1-p)([\sigma_{i,j}(t) - M]/M)$, where $p = q(a-1)$. The two thresholds have been derived from the expression of the unstable branch $\tilde{f}$ in Eq. (4).

When the jump conditions are not fulfilled, the state of the site (i,j) evolves within each separate branch, that is,

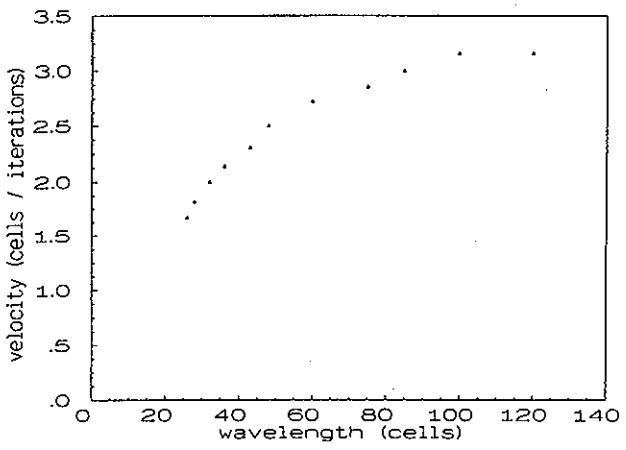

FIG. 2. Dispersion curve velocity c vs wavelength λ of the excitation, evaluated with the CA without superexcitability, with periodic boundary condition, grid size $\lambda\times\lambda$ and with the following parameters: $R=5$, $M=100$ (same for every cell), q=0.08, $G_+=0.3$, $G_-=0.2$, $\sigma_e=65$, $\sigma_d=80$. The single branch disappears below λ_{min}. CA with periodic boundary conditions. $T_{min}\equiv\lambda_{min}/c_{min}\simeq 16$ temporal steps. The tangent of the dispersion curve for $\lambda=\lambda_{min}$ approximately crosses the origin.

$$\sigma_{i,j}(t+1)=\sigma_{i,j}(t)-\text{int}[G_+(\sigma_{i,j}(t)-M+1)] \quad \text{if } \sigma_{i,j}(t)>M, \tag{10a}$$

$$\sigma_{i,j}(t+1)=\sigma_{i,j}(t)-\text{int}[G_-\sigma_{i,j}(t)] \quad \text{if } \sigma_{i,j}(t)<M. \tag{10b}$$

With this CA model, the dispersion relation between the wavelength λ and the propagation velocity c of a plane wave train has been derived. To obtain the velocity c corresponding to a chosen wavelength, simulations have been performed with $N=\lambda$ and with $\sigma(1,j)=\sigma(N,j)$, $j=1,\ldots,N$. The measurement of c has been done after a suitable transient time necessary for the system to reach its stationary state. The dispersion curve is shown in Fig. 2 and it is in good agreement with theoretical predictions.[6] Notice that Fig. 2 shows a minimal wavelength λ_{min} (thus a minimal velocity c_{min}) below which propagation fails. The period T of the plane wave train (defined as the ratio between λ and c) is the reciprocal of the slope of a straight line through the origin to the point $(\lambda,c(\lambda))$. The minimum period corresponds to the maximal slope, which arises when the straight

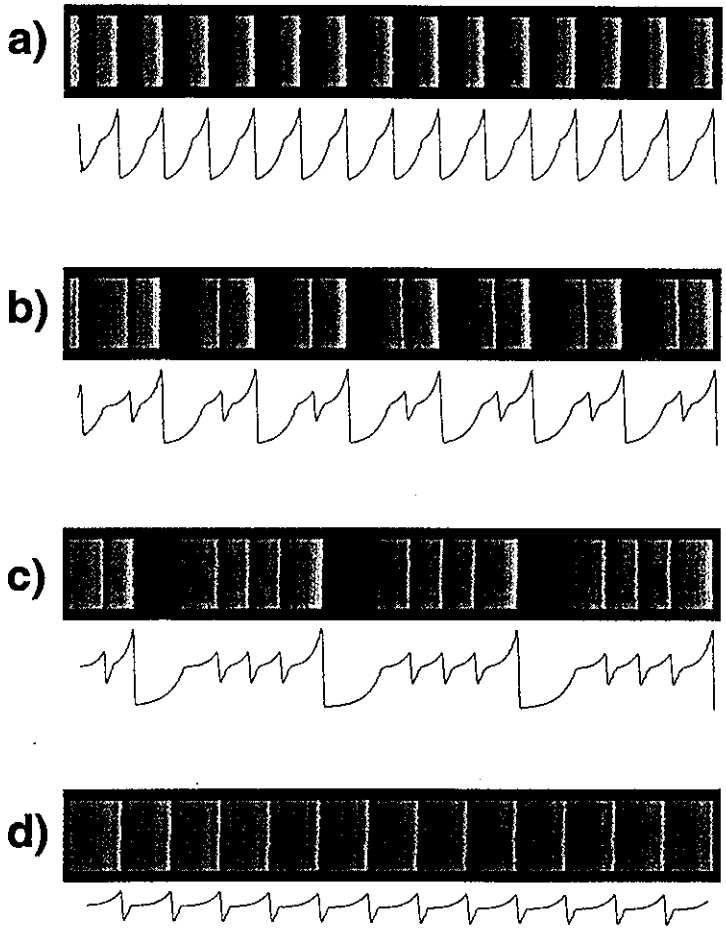

FIG. 3. Patterns of excitation (upper photos) and plots of excitation σ vs x coordinate (lower diagrams) obtained by forcing the system with a pace-maker. (a) $\tau=17$ and 16; (b) $\tau=15$ and (c) $\tau=14$ and 13. CA with no flux boundary conditions, grid 50×600, same parameters as in Fig. 2 plus a superexcitability level $\sigma_{se}=52$. When superexcitability is suppressed, a $T_{min}=18$ (different from what obtained in the caption of Fig. 2) emerges due to different boundary conditions. Grey levels are inversely proportional to σ from excited state (white) to steady state (black).

line is tangent to the dispersion curve. In Fig. 2, this occurs for $\lambda=\lambda_{min}$, and such a feature seems to be generic.[3]

Now, performing simulations with N much bigger than λ_{min}, no flux boundary conditions and an additional pace-maker which forces the system with an excitation period τ, for $\tau<T_{min}\equiv\lambda_{min}/c_{min}$, plane wavefronts are unstable and break into curls setting spiral modes. For parameters as in Fig. 2, $T_{min}\simeq 16$ temporal steps.

The CA model described above presents some advantages with respect to those described in Refs. 2 and 8. The CA introduced in Ref. 8, although it is faster, presents a dishomogeneity in spatial directions and gives rise to stair-like dispersion curves. In the model of Ref. 2 no connection with the PDE's is given in order to extract the CA evolution rules and the wave back is purely a phase wave. The connection with the CA of Ref. 2 have been pointed out above.

The aim of the present work is to apply this CA model to the dynamical behavior of an assembly of cardiac cells. The FHN model, as well as many piecewise linear relatives, have been used as proxies for normal ventricular myocardium in numerical experiments[15] with ε ranging from 0.01 to 0.001.[16] Since ε is very close to zero, the one variable treatment presented above appears most appropriate in order to minimize the computational effort.

Different cardiac cells present slightly different recovery times.[17] This has been taken into account by considering a spatial dependence of the M value and hence by redefining $M=M(i,j)$ in Eqs. (9) and (10). Furthermore, cardiac cells are characterized by the existence of a short superexcitability time interval (called "supernormal period" and later reported as supernormal interval) lying between the absolute refractory interval and the relative refractory one, and evidence of which has been recently reported.[18] Such a new feature can be easily introduced in our model by setting a new level σ_{se} such that, for $\sigma_{se}<\sigma_{i,j}(t)<\sigma_e$, the excitation threshold assumes the value $p-1$. The level σ_{se} has been chosen in such a way that every cell spends only one time step in the superexcitable state, that is, from Eq. (10b),

$$\sigma_{se}=\mathrm{int}[\sigma_e(1-G_-)]. \tag{11}$$

This new threshold value can be extracted directly by modifying the analytical form of the unstable branch $\tilde{f}$ and by enriching the FHN model with a further term as, for instance,

$$f(u,v)=u(u-1)\left(q+\frac{1-q}{M}v-u-C_1\exp\left(-\frac{[v-(\sigma_{se}+\sigma_e)/2]^2}{C_2}\right)\right), \tag{12}$$

where C_1, C_2 are suitable constants in order to obtain the desired supernormal threshold (see Fig. 1).

The supernormal interval determines crucial changes in the phenomenology for pace-maker forcing periods τ close to T_{min}, which, in this latter case, no longer represents the minimal period of propagating waves. In particular, for $\tau=17$ and 16, there is an alternation between a front of excitation following the supernormal interval and a front of excitation developing on the refractory tail, so that two different wavelengths (A and B) for the same velocity emerge. The resulting symbolic dynamics is a period 2 dynamics ($ABAB\ldots$). For $T=15$, three excitation fronts follow the supernormal interval and one evolves on the relative refractory interval. The resulting pattern consists of three short wavelengths (B,C,D) very close to each other and one longer (A). The symbolic dynamics has a period 4 ($ABCDABCD\ldots$). For $\tau=14$ and 13, excitation fronts propagate only in the supernormal interval and hence a unique wavelength (A) is obtained (symbolic dynamics: $AAA\ldots$). Figure 3 shows the obtained patterns from $\tau=17$ to $\tau=14$. Finally, for $T<13$, an instantaneous destabilization of plane fronts toward complete spatiotemporally decorrelated patterns occurs. In particular, if the CA is covered by a regular plane wave train with period $\tau>T_{min}$ and the pace-maker suddenly delivers a further forcing excitation delayed from the previous one by less than 13 (this phenomenon is known in cardiology as "extrasystole"), this latter front quickly shatters, giving rise to a fibrillating pattern without any production of spirals, as shown in Fig. 4.

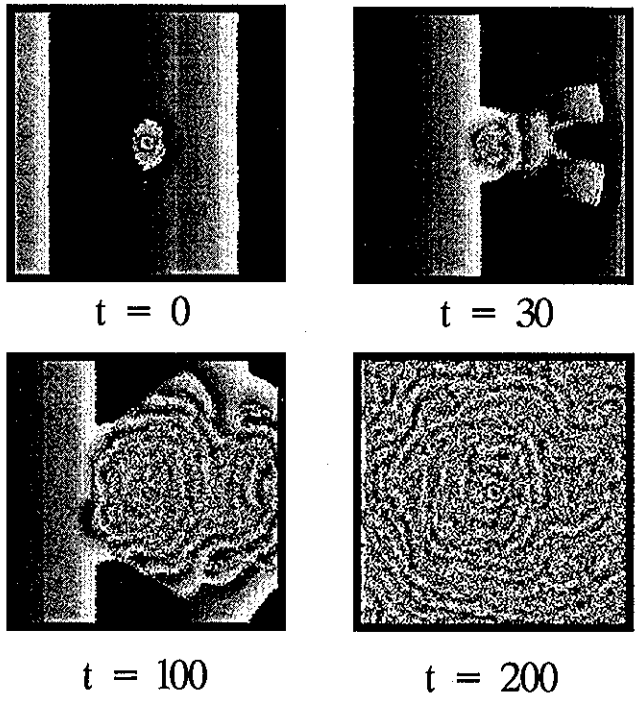

FIG. 4. Fast transition toward fibrillation. CA with same parameters and grey level stipulations as in Fig. 3. Localized pulse has been provided at $\tau=12$.

Such a phenomenology suggests two qualitatively different transitions to fibrillation. The first one (slow transition) occurs when spiral waves take place inside the cardiac tissue. For parameter values which destabilize the spirals, they break, generating other spirals. If this behavior occurs several times, we get a complete cardiac fibrillation.

The second form of transition (fast transition) often occurs in heart samples where a single pulse with an adequate timing can determine an instantaneous transition toward car-

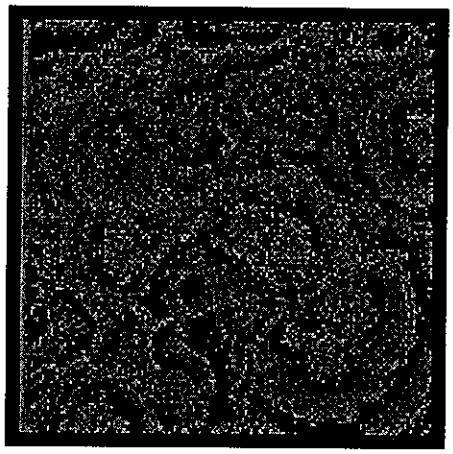

a)

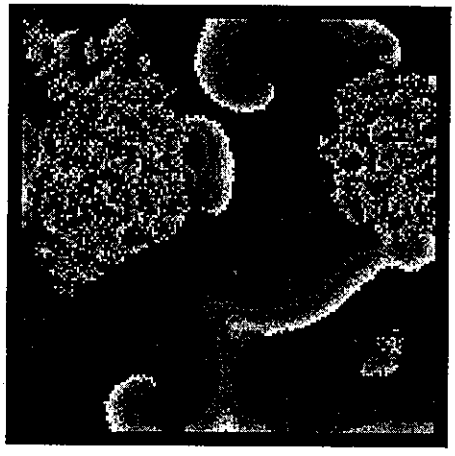

b)

FIG. 5. (a) Global fibrillation due to spatially random initial excitation; (b) local fibrillation coexisting with a quasiregular spatial dynamics, obtained by simulating a drug intervention. Thresholds modified as in the text. Same parameters and grey level stipulations as in Fig. 3.

diac fibrillation without any production of spiral modes as reproduced above. Cardiologists have observed such a transition either when the pulse is provided by a natural pacemaker (extrasystole natural mechanism[19]), or when the pulse is artificially provided in order to produce fibrillation in samples of cardiac tissue.

Independently on whether the transition is slow or fast, two types of qualitative behaviors have been observed. Precisely, starting from a spatially random initial excitation, a fibrillation covering the whole spatial domain has been obtained [Fig. 5(a)]. Then, modifying $G_{\pm}$ and p (G_+ has been increased by 0.02, G_- decreased by 0.02 and p increased by 1 for simulating qualitatively a drug intervention), fibrillation can either die or persist confined within a limited region [Fig. 5(b)], thus coexisting with a quasiregular dynamics in other parts of the frame. Such a latter case, despite its rareness, has been observed in human heart.[20]

In conclusion, we have shown how the limit $\varepsilon \to 0$ of the FitzHugh–Nagumo reaction diffusion model can be easily simulated by a single variable cellular automaton that mimics sufficiently well the behavior of EM. The further addition of a short superexcitability period permits us to correctly approach several cardiac pathologies and to explain how fast transitions to decorrelated patches can occur. However, direct simulations of the PDE's in presence of superexcitability in order to check the validity of CA approach have not been so far performed.

ACKNOWLEDGMENT

We acknowledge G.P. Puccioni for programming assistance.

[1] A. M. Zhabotinsky, Chaos **1**, 379 (1991).
[2] M. Markus and B. Hess, Nature **347**, 6288 (1990).
[3] A. T. Winfree, Chaos **1**, 303 (1991).
[4] J. J. Tyson and G. P. Keener, Physica D **29**, 215 (1987).
[5] R. N. Khramov and V. I. Krinskii, Biofizika **22**, 512 (1977).
[6] For a review on these subjects see: E. Meron, Phys. Rep. **218**, 1 (1992).
[7] B. S. Kerner and V. V. Osipov, Sov. Phys. Usp. **33**, 679 (1990).
[8] M. Gerardt, H. Schuster, and J. J. Tyson, Physica D **46**, 392 (1992).
[9] D. Barkley, Physica D **49**, 61 (1991).
[10] A. M. Pertsov, E. A. Ermakova, and A. V. Pamfilov, Physica D **14**, 117 (1984).
[11] For a review of the singular perturbation approach to this case see: J. J. Tyson and G. P. Keener, Physica D **32**, 327 (1988).
[12] D. R. Chialvo, D. C. Michaels, and J. Jalife, Circ. Res. **66**, 525 (1990).
[13] E. S. Gang, T. Peter, H. S. Karagueuzian, W. J. Mandel, and M. Meesmann, Cardiovasc. Res. **21**, 790 (1988).
[14] M. Markus (private communication).
[15] *Mathematical Approaches to Cardiac Arrhythmias,* edited by J. Jalife (New York Academy of Sciences, New York, 1990), Vol. 501, p.190.
[16] A. T. Winfree, "Estimating the Ventricular Fibrillation Threshold," in *Theory of Heart: Biomechanics, Biophysics, and Nonlinear Dynamics of Cardiac Function*, edited by L. Glass, P. Hunter, and A. McCullough (Springer-Verlag, New York, 1991), Chap. 19, p.477.
[17] B. Smawicz, "Dispersion of Refractoriness in Ventricular Arrhythmias," in *Cardiac Electrophysiology. From Cell to Bedside*, edited by D. P. Zipes and J. Jalife (Saunders, Philadelphia, 1990), Chap. 41, p. 377.
[18] D. R. Chialvo and J. Jalife, Nature **330**, 749 (1987).
[19] G. H. Bardy and W. H. Olson, "Clinical Characteristics of Spontaneous-Onset Sustained Ventricular Tachycardia and Ventricular Fibrillation in Survivors of Cardiac Arrest," *Cardiac Electrophysiology. From Cell to Bedside*, edited by D. P. Zipes and J. Jalife (Saunders, Philadelphia, 1990), Chap. 81, p. 778.
[20] J. A. Gomes, P. S. Kang, M. Matheson, W. B. Gough Jr. and N. El-Sherif, Circulation **63**, 80 (1981).